High sensitivity transient infrared spectroscopy: a UV/Visible transient grating spectrometer with a heterodyne detected infrared probe

Donaldson, Paul M ; Strzalka, Halina ; Hamm, Peter

DOI: https://doi.org/10.1364/OE.20.012761

High sensitivity transient infrared spectroscopy: a UV/Visible transient grating spectrometer with a heterodyne detected infrared probe

Paul M. Donaldson, Halina Strzalka, and Peter Hamm*

Institute of Physical Chemistry, University of Zürich, Winterthurerstrasse 190, Zürich CH-8057, Switzerland
**phamm@pci.uzh.ch*

Abstract: We describe here a high sensitivity means of performing time resolved UV/Visible pump, infrared probe spectroscopy using optically Heterodyne Detected UV-IR Transient Gratings. The experiment design employed is simple, robust and includes a novel means of generating phase locked pulse pairs that relies on only mirrors and a beamsplitter. A signal to noise ratio increase of 24 compared with a conventional pump-probe arrangement is demonstrated.

OCIS codes: (300.6530) Spectroscopy, ultrafast; (190.2055) Dynamic gratings; (120.6200) Spectrometers and spectroscopic instrumentation.

References and links

1. E. T. J. Nibbering, H. Fidder, and E. Pines, "Ultrafast chemistry: using time-resolved vibrational spectroscopy for interrogation of structural dynamics," Annu. Rev. Phys. Chem. **56**(1), 337–367 (2005).
2. J. P. Woerdman and B. Bolger, "Diffraction of light by a laser induced grating in Si," Phys. Lett. A **30**(3), 164–165 (1969).
3. J. R. Salcedo, A. E. Siegman, D. D. Dlott, and M. D. Fayer, "Dynamics of energy-transport in molecular-crystals - picosecond transient-grating method," Phys. Rev. Lett. **41**(2), 131–134 (1978).
4. T. H. Joo, Y. W. Jia, J. Y. Yu, M. J. Lang, and G. R. Fleming, "Third-order nonlinear time domain probes of solvation dynamics," J. Chem. Phys. **104**(16), 6089–6108 (1996).
5. G. D. Goodno, G. Dadusc, and R. J. D. Miller, "Ultrafast heterodyne-detected transient-grating spectroscopy using diffractive optics," J. Opt. Soc. Am. B **15**(6), 1791–1794 (1998).
6. A. A. Maznev, K. A. Nelson, and J. A. Rogers, "Optical heterodyne detection of laser-induced gratings," Opt. Lett. **23**(16), 1319–1321 (1998).
7. M. J. Ammend and D. A. Blank, "Passive optical interferometer without spatial overlap between the local oscillator and signal generation," Opt. Lett. **34**(4), 548–550 (2009).
8. C. Khurmi and M. A. Berg, "Differential heterodyne detection with diffractive optics for multidimensional transient-grating spectroscopy," J. Opt. Soc. Am. B **26**(12), 2357–2362 (2009).
9. J. P. Ogilvie, M. Plazanet, G. Dadusc, and R. J. D. Miller, "Dynamics of ligand escape in myoglobin: Q- band transient absorption and four-wave mixing studies," J. Phys. Chem. B **106**(40), 10460–10467 (2002).
10. R. Bloem, S. Garrett-Roe, H. Strzalka, P. Hamm, and P. Donaldson, "Enhancing signal detection and completely eliminating scattering using quasi-phase-cycling in 2D IR experiments," Opt. Express **18**(26), 27067–27078 (2010).
11. G. L. Eesley, M. D. Levenson, and W. M. Tolles, "Optically heterodyned coherent Raman-spectroscopy," IEEE J. Quantum Electron. **14**(1), 45–49 (1978).
12. A. Owyoung, "Coherent Raman gain spectroscopy using CW laser sources," IEEE J. Quantum Electron. **14**(3), 192–203 (1978).
13. J. Réhault, V. Zanirato, M. Olivucci, and J. Helbing, "Linear dichroism amplification: adapting a long-known technique for ultrasensitive femtosecond IR spectroscopy," J. Chem. Phys. **134**(12), 124516 (2011).
14. P. Hamm, R. A. Kaindl, and J. Stenger, "Noise suppression in femtosecond mid-infrared light sources," Opt. Lett. **25**(24), 1798–1800 (2000).
15. U. Selig, F. Langhojer, F. Dimler, T. Löhrig, C. Schwarz, B. Gieseking, and T. Brixner, "Inherently phase-stable coherent two-dimensional spectroscopy using only conventional optics," Opt. Lett. **33**(23), 2851–2853 (2008).
16. J. Bredenbeck, J. Helbing, and P. Hamm, "Transient two-dimensional infrared spectroscopy: exploring the polarization dependence," J. Chem. Phys. **121**(12), 5943–5957 (2004).
17. M. L. Cowan, B. D. Bruner, N. Huse, J. R. Dwyer, B. Chugh, E. T. J. Nibbering, T. Elsaesser, and R. J. D. Miller, "Ultrafast memory loss and energy redistribution in the hydrogen bond network of liquid H2O," Nature **434**(7030), 199–202 (2005).
18. L. DeFlores, "Multi-mode two-dimensional infrared spectroscopy of peptides and proteins," in *PhD Thesis* (Massachusetts Institute of Technology, 2008).

#162266 - $15.00 USD Received 31 Jan 2012; accepted 21 Mar 2012; published 23 May 2012

1. Introduction

Transient infrared spectroscopy is a useful tool for studying fast and ultrafast nonequilibrium processes in a wide variety of condensed phased systems. Spectra are recorded by exciting a sample with an ultraviolet (UV)/visible pump laser pulse and recording an infrared (IR) spectrum of the excited sample with a probe pulse. Through the chemical information available from IR spectroscopy, such 'pump-probe' measurements are commonly used to follow photochemical processes, detect reactive intermediates and characterize excited-state structural dynamics, solvation dynamics and relaxation processes. The breadth and depth of the field was recently covered in an extensive review [1].

The range of possible chemical applications of infrared pump-probe spectroscopy is limited to samples which show infrared absorbance changes after pumping that are larger than 10^{-6}-10^{-5}, or 1-10 μOD. Our interest is in measuring transient infrared spectra from single labels in proteins. To measure transient infrared spectra from an azide or cyano label in a protein, a high sample concentration of ~10 mM would be required, problematic both in terms of the quantities of labeled protein needed and steady-state protein stability. Such samples can also be quickly lost during the measurement process as a result of photo-degradation and the production of unstable species in the laser spot can result in material building up on the sample cell windows. These two effects necessitate lowering the pump energy, and therefore the signal size.

In this paper, we present a solution to the above problems using a new means of measuring UV/Vis – IR pump probe spectra, which, compared with an optimised pump-probe setup gives > 20 times improvement in signal to noise. This improvement is achieved by using a *heterodyne detected infrared probe generated from a UV or visible transient grating*. For notational simplicity we denote the method as Optically Heterodyne Detected UV-IR Transient Grating spectroscopy (OHD-UV-IR TG spectroscopy). To demonstrate the performance and characteristics of this method, transient grating spectra from a model Rhenium-carbonyl system are presented.

Transient grating spectroscopy has a long history of development in the visible part of the spectrum, both decades ago [2–6] and also more recently [7, 8]. The use of diffractive optics has simplified considerably the design of simple and robust spectrometers [5, 6, 9]. The experiment presented here incorporates a number of unique features. Whilst the phase-locked infrared pulses are generated from a diffractive optic made in-house, phase-locked pairs of UV pulses are generated using a simple optical arrangement comprising only three mirrors and a beamsplitter. The flexibility afforded by this method greatly simplifies matching the widely differing Bragg angles of the UV and mid-IR pulses. A simple experimental geometry allows for heterodyned infrared transient grating signals to be measured in a balanced arrangement, which in a similar manner to that described in [9], readily gives absorptive spectra in a phase stable manner. An additional improvement in signal to noise is achieved by using a quartz wobbler [10] to modulate the transient grating phase.

In the language of nonlinear spectroscopy, the transient grating technique generates a background-free signal in a four wave mixing geometry through phase matching. Another important type of method for heterodyne detection of background-free nonlinear signals is possible when a pump beam induces polarization *anisotropy* in the sample. Then, a polariser in the probe can be used to 'leak' a local oscillator field onto a detector, collinear with the signal [11, 12]. A UV/Visible pump, IR probe technique based on these principles was recently demonstrated by *Helbing* et al. [13], showing more than an order of magnitude enhancement in the anisotropic component of the UV pump, IR probe signal. Such an experiment is an alternative to transient grating spectroscopy with the advantage that it requires only the insertion of polarizers (albeit of high quality) into any existing pump-probe setup. We show here that OHD-UV-IR TG spectroscopy need not be a significant departure in complexity from pump-probe spectroscopy. As one can measure both isotropic and anisotropic signals, it is also applicable to a wider range of measurements than OHD techniques based on anisotropy.

#162266 - $15.00 USD Received 31 Jan 2012; accepted 21 Mar 2012; published 23 May 2012

2. Background: pump-probe spectroscopy versus transient grating spectroscopy

We first briefly explore why a heterodyne detected transient grating experiment can give a higher signal to noise in a transient infrared measurement compared with a conventional pump-probe arrangement. Pump-probe and heterodyned transient grating spectroscopy are of course related by the same response function formalism; the information is just read out in different ways, with the imaginary (absorptive) part of the transient grating response identical to the pump-probe response.

Consider two fields that mix on a square-law detector. We denote them as 'local oscillator' (*LO*) and 'signal'. The measured intensity follows:

$$I \propto E_{LO}^2 + E_{sig}^2 + 2E_{LO}E_{sig}\cos(\omega\Delta t + \delta) \qquad (1)$$

This well known expression describes the interference between the two fields. The interference term can be positive or negative depending on the phase difference δ between the two fields. If the fields are pulsed, the relative pulse timing Δt also enters in the interference term.

For the case of a pump-probe experiment, the weak signal is radiated in the same direction as the probe. The probe both drives the signal and acts as the *LO*. The minimum infrared absorbance change that can be measured is therefore determined by the noise of the probe (through the large E_{LO}^2 term). There is no way to increase the signal without increasing the noisy E_{LO}^2 term. For the transient grating geometry, the probing and heterodyne detection steps are separate. The ± 1 order transient grating signals do not contain any light from the infrared probe, which excluding scatter, propagates separately as the zero order diffracted beam. The local oscillators used to detect the third order signal are then added separately. Thus, unlike conventional pump-probe spectroscopy, the heterodyne transient grating signal to noise ratio can be optimised using the largest possible intensities for both the probe and the additional local oscillators.

Based on typical experimental parameters, we can estimate the expected signal to noise gain in an OHD-UV-IR TG experiment. The HgCdTe (MCT) array detectors used to detect infrared light become laser noise limited above the range of ~2-20 nJ undispersed incident infrared energy per pulse. Therefore a pump-probe or transient grating experiment will typically use these levels for the probe or local oscillator. An OPA generating infrared light through difference frequency generation however produces around 2 μJ per pulse. Most of this energy can be used in the transient grating experiment as the probe. This 100-1000 times increase in infrared energy incident on the sample represents a 10-30 times increase in field strength and therefore signal size. Phase modulation instead of amplitude modulation (chopping) gives an extra factor of two. Therefore the expected improvement in signal to noise compared with pump-probe is in the range of 20-60.

3. OHD-UV-IR TG spectroscopy: experiment

For generating the mid-IR light used as a probe in the experiment, a regenerative amplifier (Spitfire XP Pro, 800 nm, ~75 fs, 5 kHz) is used to pump an optical parametric amplifier, which via difference frequency mixing in $AgGaS_2$, generates infrared light with ~2025 cm^{-1} centre wavelength and ~2 μJ / pulse [14]. The UV excitation pulses (~0.2 – 1.5 μJ / pulse) are generated from the second harmonic of the 800 nm light.

Figure 1 shows a simplified schematic of the experiment. A phase-locked UV pulse pair (1) is focused (f = 75 cm) to a width ($1/e^2$) of 140 μm in the sample of interest (2), forming the population grating. An infrared beam (3) is focused onto a CaF_2 diffractive optic (4), prepared using a simple line burning process as described in the appendix. The zero order beam (referred to as the probe) and ± 1 order beams (the local oscillators, 0.1 - 1% of the probe intensity) are relayed to the sample via a pair of 12.25 cm focal length off-axis parabolic mirrors (giving a probe focal width at the sample of 120 μm). Diffractive optic line densities of ~20-40 mm^{-1} are used in order to give ± 1 order separations of 2-4 cm on the parabolic

#162266 - $15.00 USD Received 31 Jan 2012; accepted 21 Mar 2012; published 23 May 2012

mirrors. The probe and local oscillator beams pass through vertically-mounted CaF_2 Brewster windows (5) which are rotated to adjust the relative delays of each beam. All infrared beams overlap with the UV transient grating in the sample. The probe beam interacts with the UV excited population grating at the sample, generating ± *1* order diffraction orders (the transient grating signals), which are imaged, dispersed in a monochromator and then re-imaged onto two separate 32 element HgCdTe (MCT) arrays.

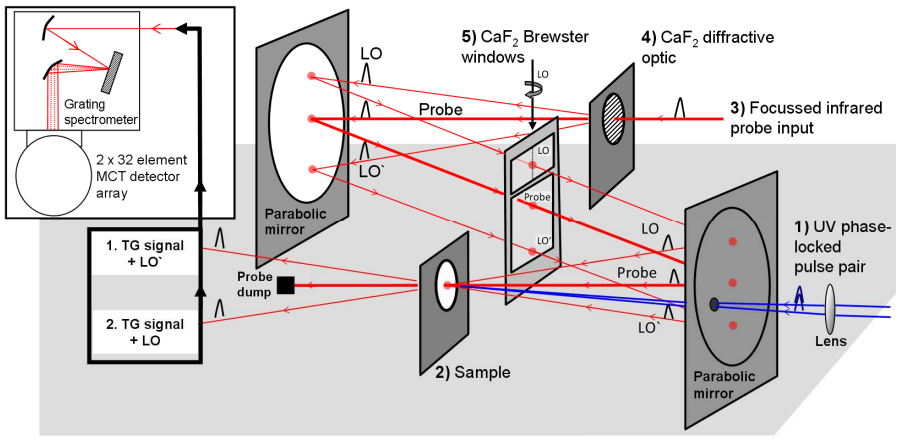

Fig. 1. The optical layout of the OHD-UV-IR TG experiment.

A key feature of this optical layout is as follows. If the line spacing of the CaF_2 diffractive optic matches the line spacing of the UV/Visible population grating, the local oscillators generated by the CaF_2 diffractive optic will emerge from the sample in the same direction as the transient grating signals, allowing heterodyne signals to be measured on the two MCT arrays. In a similar manner to [9], the two signal phases can be adjusted so that the difference gives an absorptive spectrum and the dispersive and homodyne E_{LO}^2 terms cancel, resulting in a reduction in noise. Each local oscillator beam also acquires a pump-probe signal, which is removed in the difference measurement, but is useful for diagnostic purposes.

4. Phase locked UV/visible pulses without diffractive optics

Phase stability (or more precisely, pathlength stability) between the pair of pulses that generate the population grating is a key requirement of any heterodyne detected grating experiment [5, 6]. Likewise, the probe and *LO* beams must have a fixed relative phase. Phase-stable one and two color OHD-TG measurements in the UV/Visible part of the spectrum can be elegantly achieved using a single diffractive optic element for pump and probe beams [9]. Due to the different material and diffraction efficiency requirements of infrared and UV/Visible light however, a single diffractive optic element for both infrared and UV pulses is not practical. The large difference in diffraction angles and focused spot sizes also mean that separate diffractive optic elements and imaging optics are preferable.

Due to the low diffraction efficiency requirements for the infrared local oscillator beams, simple line burned diffractive optic elements described in Appendix 1 are used for the probing side of the experiment. On the pump side however, greater diffraction efficiency into the ± *1* orders is required, necessitating more sophisticated grating fabrication methods. Instead of using a diffractive optic for this step, in this paper we present an alternative means of generating phase-locked optical pulses which works through a simple arrangement of mirrors and a beamsplitter.

#162266 - $15.00 USD Received 31 Jan 2012; accepted 21 Mar 2012; published 23 May 2012

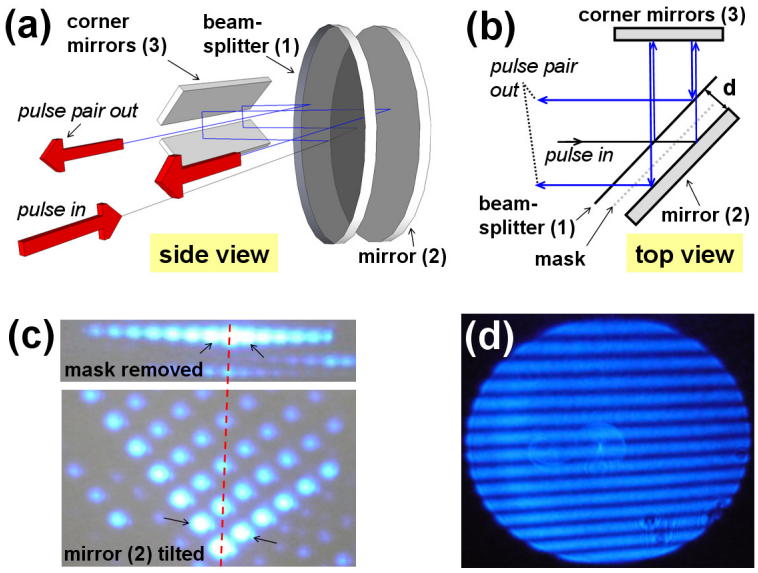

Fig. 2. A simple scheme for generating phase locked pulse pairs. (a) Side view of the optics used. (b) Top view. (c) Multiple reflections from the pulse pair generator, observed by removing the masks and introducing a vertical tilt on mirror (2). The pulse pair indicated by the black arrows is used in OHD-TG measurements: it is phase locked and contains 25% of the incident light. The weaker (and later) pulse pairs lying symmetrically about the vertical axis (red line) are also temporally synchronized. The very faint spots are reflections from the front surface of the beamsplitter. (d) Fringes generated using the pulse pairs via 400 nm light focused at the sample position (see Fig. 1) and imaged with a microscope objective.

Figure 2(a) and 2(b) shows the optical design. It comprises a 50/50 beamsplitter (1) and a mirror (2) separated by distance *d*. A corner retro-reflector returns the beams back through the beamsplitter with a vertical offset. This arrangement generates multiple reflections from a 45° incident beam, as shown in Fig. 2(c). Two reflections are of particular interest, as shown in Fig. 2(b). These reflections both pass through and reflect off the beamsplitter once and reflect off each mirror once. They therefore have perfectly correlated timings and comprise 25% of the incident intensity. A mask between the beamsplitter (1) and mirror (2) and a mask on the exit of the device is used to isolate these reflections. Upon focusing, the pair generates stable fringes, as shown in Fig. 2(d). The fringe spacing is adjusted simply by changing the distance *d* between the mirror and the beamsplitter. In practice, the separation of the pulse pair is set to give fringes at the sample position calculated for a given focal length to match those of the infrared diffractive optic.

As a side remark, for experiments where 25% pulse pair generation efficiency is not sufficient, we suggest two ways here of making this method close to 100% efficient. The first is to pattern 50/50, transmissive and reflective sections onto the beamsplitter in a manner that eliminates all other reflections, as shown in Fig. 3(a). Alternatively, an arrangement of quarter-waveplates and a polarizing beamsplitter shown in Fig. 3(b) can be used to give phase-locked *orthogonally polarized* pulses, again with 100% efficiency.

#162266 - $15.00 USD
Received 31 Jan 2012; accepted 21 Mar 2012; published 23 May 2012

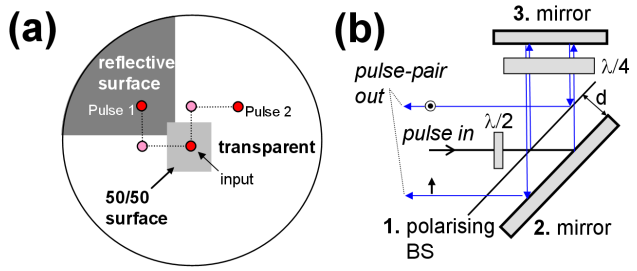

Fig. 3. Increasing the efficiency of the phase locked pulse pair generation scheme. (a) shows a patterned beamsplitter designed to eliminate all unwanted reflections. The red (dark) circles indicate where the input and output beams pass through/reflect from the beamsplitter. The pink (light) circles represent the intermediate reflections involving mirror (2). In (b), a 100% efficient method based on polarizers is shown. 45° linearly polarized light is split by a polarizing beamsplitter. The reflected and transmitted portions propagate twice through a λ/4 waveplate, inverting their polarisations and giving the correct phase locked pair after a second pass over the beamsplitter.

In a typical transient infrared experiment, the incident pump beam is usually routed to the sample via a motorized delay stage with up to 30 cm travel. There are inevitably small changes in beam alignment when scanning such a delay stage. For a motorized stage placed before the pulse-pair generator, the resulting change in pathlength appears identically in each pulse. The interference fringes generated by the arrangement in Fig. 3 therefore do not change when the input beam pointing is varied.

It is worth noting that the simple means of producing phase locked pulse pairs demonstrated in this paper using only mirrors and a beamsplitter can be considered as a useful alternative to diffractive optics-based methods for a variety of nonlinear optical experiments. We note that phase stability in heterodyne detected boxcars 2D spectroscopy using only beamsplitters and mirrors has previously been achieved [15], however the arrangement does not produce pairs of pulses that are phase stable. A stable phase for the heterodyned third order 2D signal ($\phi_{het} = \phi_1 - \phi_2 + \phi_3 - \phi_{LO}$) is instead obtained by a clever cancellation of fluctuations across all four beams. Although this method is an excellent solution for single colour 2D experiments, for a two colour experiment, the cancellation does not occur. A 2D electronic or infrared experiment could feasibly be constructed using two phase locked pair generators, giving a mirror/beamsplitter setup that allows pump (E_1 and E_2) and probe (E_1 and E_{LO}) pulses to have different centre wavelengths.

5. Doubling signal to noise using pseudo-phase modulating wobblers

Isolation of the UV-IR heterodyned transient grating signal $2E_{SIG}\ E_{LO}$ from the E_{LO}^2 background (Eq. (1)) can in principle be achieved using the conventional method of optically chopping the UV pump at half the laser repetition rate and subtracting successive shots (as is done in most kHz rate pump-probe experiments). This inevitably means that half of the laser shots do not contain any transient grating signal. If instead, the phase of the signal is modulated on a shot by shot basis, subtraction of successive shots *doubles* the signal for the same noise (based on the fact that E_{LO}^2 is the dominant noise source).

In a recent publication [10], we introduced simple, easily fabricated devices for modulating laser pulse timing on a shot by shot, sub-optical cycle level which we termed 'wobblers'. For modulating the phase of the transient grating signal in the experiment described in this paper, a 2.5 kHz Brewster angle, 2mm thick quartz wobbler driven with a 5 mm diameter steel tube resonator is used in one of the phase-locked 400 nm pump beams to modulate the phase of the UV/Visible population grating, φ_{TG}. An identical window is placed in the other 400 nm pump beam as compensation. Driven by pulses synchronized to half the laser repetition rate ($\nu_{1/2}$), the Brewster window of a wobbler moves in a sinusoidal motion. The correct wobbler drive phase (relative to the laser trigger) is found by first modulating the transient grating signal with an arbitrary amplitude and adjusting the drive phase until the

#162266 - $15.00 USD Received 31 Jan 2012; accepted 21 Mar 2012; published 23 May 2012

signal is zero. With this phase, every laser pulse crosses the wobbler at its equilibrium position and the correct drive phase shift can then be achieved by adding an extra phase of ± $\pi/2$ ($1/v_{1/2}$ delay). Finding the correct drive level is then a matter of adjusting the amplitude until the difference transient grating signal is maximized. The difference transient grating signal is then calculated for each pixel in logarithmic ('absorbance') units as:

$$Signal = Log_{10} \frac{S^{+}_{array\,1} S^{-}_{array\,2}}{S^{-}_{array\,1} S^{+}_{array\,2}} \tag{4}$$

6. Results

In this section, we present OHD-UV-IR TG data from a model chemical system, Re(CO)3(dmbpy)Br (dmbpy = 4,4'dimethyl 2,2' bipyridine) and discuss the experimental performance in terms of signal to noise.

$Re(CO)_3$(dmbpy)Br was used dissolved in DMSO. Metal-to-ligand charge transfer in this compound is driven using 400 nm pump light, giving clear infrared carbonyl-stretch ground-state bleach/excited state absorption transients. Using appropriate sample concentrations, pathlengths and pulse energies, the experimental arrangement in Fig. 1 allows conventional pump-probe signals from $Re(CO)_3$(dmbpy)Br to be measured. In our setup these were comparable in size to previously published spectra [16] and could therefore be used to determine the level of signal enhancement obtained when detecting the heterodyned transient grating signal.

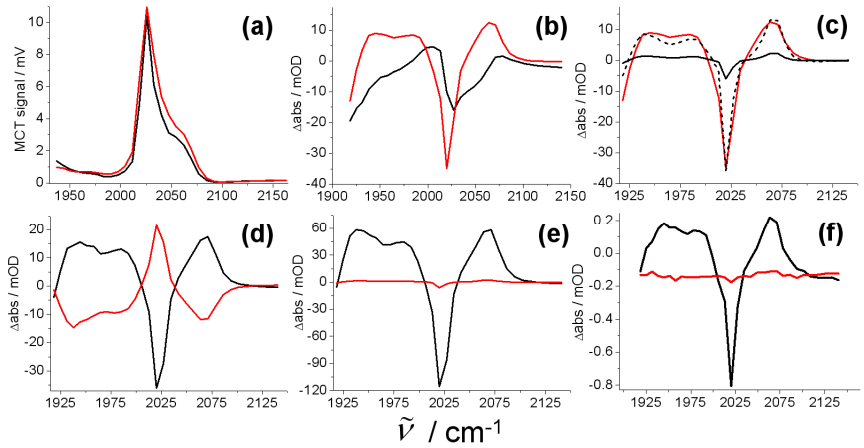

Fig. 4. $Re(CO)_3$(dmbpy)Br transient spectra measured using the OHD-UV-IR TG experiment. (a) Homodyne TG signals measured on the two MCT arrays. (b) The absorptive (red) and dispersive (black) components of the heterodyned grating signal on a single MCT array. (c) The array 1 absorptive transient grating signal (red) compared with the pump-probe signal (solid black). The pump probe signal is magnified by x6 (dotted line) to match the transient grating signal. (d) The absorptive transient grating signal measured on both arrays, but with opposite signs. (e) The difference of signals in (d) and the use of an optical wobbler gives a 24x increase in absorptive transient grating signal (black) compared with pump-probe signal (red). (f) The absorptive transient grating signal (black) and pump-probe signal (red) from a 20 μM $Re(CO)_3$(dmbpy)Br solution. All spectra were recorded with 1 s signal averaging.

Figure 4 shows $Re(CO)_3$(dmbpy)Br transient spectra which illustrate the features of the OHD-UV-IR TG experiment. Figure 4(a) shows the ± *1* orders of the homodyne transient grating signal, obtained by simply blocking the local oscillator beams. Unblocking the local oscillators and detecting the heterodyne term by chopping, or wobbling gives the signals shown in Figs. 4(b)–4(f). On a single array, the signal can be changed from dispersive to absorptive (Fig. 4(b)) simply by translating the diffractive optic.

Comparison of the absorptive transient grating signal with the pump-probe signal on the local oscillators show that the heterodyned transient grating signal is typically ~4-6 times

#162266 - $15.00 USD Received 31 Jan 2012; accepted 21 Mar 2012; published 23 May 2012

bigger than the pump-probe signal for the same noise (Fig. 4(c)). This enhancement depends on the energy in the infrared probe pulse and on the overlap between the transient grating signals and the local oscillators. We believe that both of these parameters can be improved upon in future experiments. Taking the difference between the out of phase absorptive signals (Fig. 4(d)) and using a wobbler instead of a chopper, we arrive at a signal enhancements in the range of 16-24x. This is shown in Fig. 4(e) for a ~5 mM $Re(CO)_3(dmbpy)Br$ solution. Figure 4(f) shows that the signal to noise is still adequate using a 1 second data acquisition time for a sample dilution of 300 times (giving ~20 μM concentration).

7. Absorptive spectra and phase stability

The experimental geometry for OHD UV-IR TG spectroscopy presented in this paper has a number of advantageous features. In this section we focus on the consequences of measuring both of the ± *1* diffraction order heterodyned transient grating signals. By taking their difference, not only do the homodyne terms (E_{LO}^2) and a proportion of their noise cancel, but any phase errors leading to dispersive contributions in the signal are cancelled, giving purely absorptive spectra with phase fluctuations on individual arrays converted to intensity fluctuations in the difference signal. This extremely useful result was first discussed and demonstrated by Ogilvie, Miller and associates for a two colour visible transient grating experiment [9] and significantly improves the robustness and ease of use of OHD TG spectrometers.

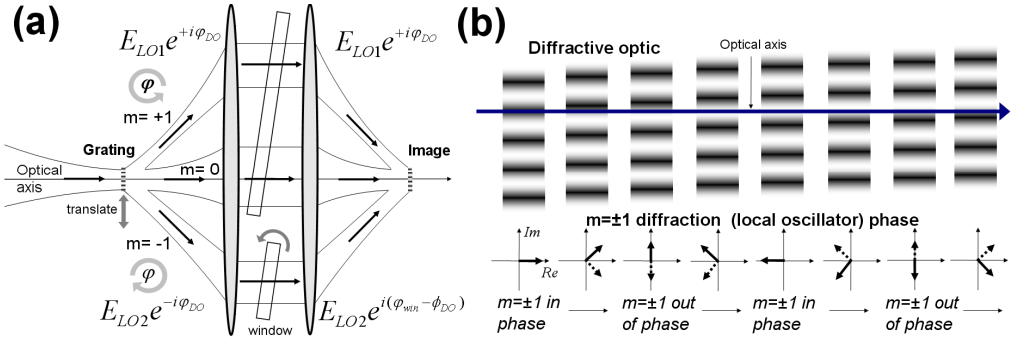

Fig. 5. (a) A depiction of the infrared beams and optics used in the OHD-UV-IR TG experiment along with the phases of the local oscillator beams. (b) A pictorial approach to understanding the relative phase changes of the ± *1 order* diffraction orders (local oscillators) when translating the diffractive optic.

For the OHD UV-IR TG experiment reported in this paper, although the overall result of differential detection is the same as [9], the fact that the phases of the UV excitation beams and infrared local oscillators are no longer related needs to be accounted for. Relative to the zero order infrared probe beam, we denote the temporal phase imparted by the diffractive optic to the ± *1* order IR heterodyne beams as φ_{DO}. The phases of the transient grating signals are set by the phase of the UV population grating and are defined as φ_{TG}. We ignore the small amount of spatial dispersion generated by the diffractive optic and population grating.

It is important to note that when a diffraction grating is spatially translated perpendicular to the optical axis, the phases of the ± *1* diffraction orders evolve in opposite directions as $\pm\varphi$. This can be understood by considering the 2*f* geometry depicted in Fig. 5(a). The image grating is a replica of the object grating and if we centre a diffraction grating symmetrically on the optical axis, as is shown in Fig. 5(b), the two diffracted orders must have the same phase relative to the zero order beam. Translating the grating breaks this symmetry and thereby causes the phases of the ± *1* diffraction orders to evolve in opposite directions. For the case when pump and probe beams are generated from the same diffractive optic, translating the diffractive optic has no effect, as φ_{DO}-φ_{TG} is constant for all grating positions.

#162266 - $15.00 USD Received 31 Jan 2012; accepted 21 Mar 2012; published 23 May 2012

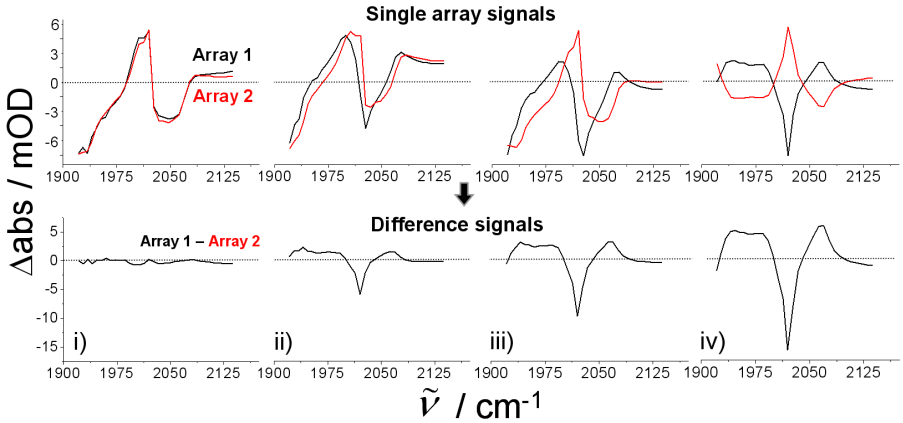

Fig. 6. Purely absorptive difference signals. Shown in i)-iv) are experimental $Re(CO)_3(dmbpy)Br$ single array signals and difference signals for different positions of the infrared diffractive optic (different values of φ_{DO}). The single array signals go from i) purely dispersive to iv) purely absorptive, whereas the difference data is always absorptive.

Combining all relevant phase terms in the OHD UV-IR TG experiment, the intensities on the MCT array detectors 1 and 2 are:

$$I_{Array\,1} \propto \left| E_{LO\,1} e^{i\phi_{DO}} + E_{TG\,1} e^{i\phi_{TG}} \right|^2 \qquad I_{Array\,1} \propto \left| E_{LO\,2} e^{i(\phi_{win} - \phi_{DO})} + E_{TG\,2} e^{-i\phi_{TG}} \right|^2 \quad (2)$$

An adjustable window is used in the experiment to add an additional pseudo-phase to *LO2* of $\varphi_{win} = \omega\Delta t$ (see Figs. 1 and 5(a)). The infrared TG signal field E_{TG} comprises dispersive (real) and absorptive (imaginary) components, $E_{TG} = E_{Disp} + iE_{Abs}$. These components both appear in the intensity expressions of Eq. (2) and are modulated through changes φ_{LO}, φ_{TG} and φ_{win}. This can be seen in the single array experimental data of Fig. 6. Assuming that the local oscillator and signal fields on arrays 1 & 2 have the same values E_{LO} and E_{TG} (i.e $E_{LO\,1} = E_{LO\,2}$, $E_{TG\,1} = E_{TG\,2}$), the difference in signals $I_{Array\,1} - I_{Array\,2}$ reduces to the following expression:

$$I_{Array\,1} - I_{Array\,2} \propto 4E_{LO}\,(E_{Disp} \sin\frac{\phi_{win}}{2} - E_{Abs} \cos\frac{\phi_{win}}{2})\ \sin(\frac{\phi_{win}}{2} - \phi_{DO} + \phi_{TG}) \quad (3)$$

Upon close examination of Eq. (3), it can be seen that by choosing $\varphi_{win} = 0$, the dispersive component of the signal disappears, independent of φ_{DO} and φ_{TG}. This interesting result means that the difference signal can be made purely absorptive, with magnitude determined by $sin(\varphi_{TG} - \varphi_{DO})$. The absorptive signal can then be maximized simply by translating the diffractive optic (optimizing φ_{DO}). This is illustrated through the experimental difference signals shown in Fig. 6. There is clearly no dispersive component in the data. $\varphi_{win} = 0$ can be found initially by using a pinhole or by using a reference sample pump-probe spectrum. Alternatively, by tuning φ_{win} and φ_{DO} together, $\varphi_{win} = 0$ can be found as a signal global minimum (Fig. 6(i)). The important point is that once located, the window angle setting does not drift significantly over time. In the single array experimental data, small phase fluctuations are observed over a timescale of hours, giving a slight dispersive component to the absorptive signal. These components perfectly cancel in the difference spectrum because they change φ_{DO} and not φ_{win}. They are most likely due to small infrared beam pointing changes on the diffractive optic.

8. Conclusions

Whilst retaining experimental simplicity, this paper extends the methodology of diffractive optic based OHD-TG spectroscopy to an important class of measurements in modern physical chemistry; transient infrared spectroscopy of optically excited chemical species. The ease of obtaining absorptive spectra and the robustness against phase drifts arising from the differential detection of ± *1* order heterodyned grating signals is a key and enabling feature of

#162266 - $15.00 USD Received 31 Jan 2012; accepted 21 Mar 2012; published 23 May 2012

the spectrometer design presented in this paper. Compared with an equivalent pump-probe experiment, the 24x increase in signal to noise demonstrated gives a ~600x decrease in the required measurement time. Further improvements in this figure are possible through higher OPA pulse energies and by improving the overlap of the local oscillator and signal fields at the detector.

Appendix. Infrared diffractive optics

As shown in Fig. 1, heterodyne detection of the two UV-IR ± 1 order transient grating signals is achieved using two local oscillator beams generated by focusing the infrared probe through a diffractive optic. Ideally the *LO* intensity should be matched to the dynamic range of the MCT detector arrays, with 0.1-1% of the 2 μJ infrared probe intensity typically used.

Phase stable *pump beam* infrared diffractive optic experiments typically require diffraction gratings with high diffraction efficiency, making gratings for diffractive optics-based 2D-IR experiments [17,18] specialized and costly items. Because of the low amounts of diffracted light required in the UV-IR transient grating experiment, the generation of phase locked infrared pulses used for the probe is met by a simple pattern burning process.

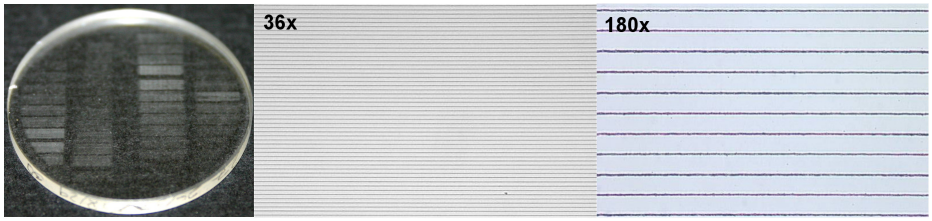

Fig. 7. Line burned diffractive optical elements on CaF_2 used for OHD UV-IR TG spectroscopy. On the left shows a window with a range of gratings periods and depths. The zooms show a particular grating with 22 μm line spacing.

Diffractive optics with 20 to 40 lines/mm were made on an optical bench by raster scanning a CaF_2 window on a computer controlled *x-y* stage in the vicinity of a tightly focused 800 nm beam (a 6.3x/0.2 microscope objective and < 1 μJ / pulse were used). Care was taken to mount the window and stages so that the window scanned perpendicular to the laser focus. This form of etching through self-focusing and dielectric surface breakdown created tracks of ~1-3 μm width. The *x-y* stages used did introduce small geometric artifacts in the grating pattern, however the accuracy of the gratings was adequate for the purposes of the OHD-UV-IR TG experiment. Ideal ranges of intensity, focusing and scan speed were found by trial and error. On a single 1 inch CaF_2 window, 20-30 gratings with different linewidths and line spacings could be drawn, allowing the local oscillator intensities and dispersion to be readily adjusted (Fig. 7). The transmitted $m=0$ beam exhibited losses of only 5%.

Acknowledgments

We would like to thank Jan Helbing for suggesting optical arrangements for polarized phase locked pulses along with Sean Garrett-Roe and RJ Dwayne Miller for helpful discussions. This work was supported by an advanced ERC investigator grant (DYNALLO) to PH and by the Swiss National Science Foundation through the NCCR network 'MUST'.